Published in final edited form as:
Neuroscience. 2007 June 29; 147(2): 354–372.

Glutamate receptor abnormalities in the YAC128 transgenic mouse model of Huntington's disease

Caroline L. Benn, Ph.D.[1], **Elizabeth J. Slow, Ph.D.**[2], **Laurie A. Farrell, RN**[1], **Rona Graham, Ph.D.**[2], **Yu Deng, B.Sc.**[2], **Michael R. Hayden, M.D., Ph.D.**[2], and **Jang-Ho J. Cha, M.D., Ph.D.**[1,*]

1 *MassGeneral Institute for Neurodegenerative Disease, Department of Neurology, Massachusetts General Hospital, 114 16th Street, Charlestown, MA 02129-4404*

2 *Centre for Molecular Medicine and Therapeutics, Department of Medical Genetics, University of British Columbia, Vancouver, British Columbia, Canada V5Z 4H4*

Abstract

A yeast artificial chromosome (YAC) mouse model of Huntington's disease (YAC128) develops motor abnormalities, age-dependent striatal atrophy and neuronal loss. Alteration of neurotransmitter receptors, particularly glutamate and dopamine receptors, is a pathological hallmark of Huntington's disease. We therefore analyzed neurotransmitter receptors in symptomatic YAC128 Huntington's disease mice. We found significant increases in NMDA, AMPA and metabotropic glutamate receptor binding, which were not due to increases in receptor subunit mRNA expression levels. Subcellular fractionation analysis revealed increased levels of glutamate receptor subunits in synaptic membrane fractions from YAC128 mice. We found no changes in dopamine, GABA or adenosine receptor binding, nor did we see alterations in dopamine D1, D2 or adenosine A2a receptor mRNA levels. The receptor abnormalities in YAC128 transgenic mice thus appear limited to glutamate receptors. We also found a significant decrease in preproenkephalin mRNA in the striatum of YAC128 mice, which contrasts with the lack of change in levels of mRNA encoding neurotransmitter receptors. Taken together, the abnormal and selective increases in glutamate receptor subunit expression and binding are not due to increases in receptor subunit expression and may exert detrimental effects. The decrease in preproenkephalin mRNA suggests a selective transcriptional deficit, as opposed to neuronal loss, and could additionally contribute to the abnormal motor symptoms in YAC128 mice.

Keywords

in situ hybridization; receptor binding; subcellular fractionation; preproenkephalin; NMDA receptor; AMPA receptor

Huntington's disease (HD) is a fatal, autosomal dominant neurodegenerative disorder for which there is no effective treatment. The causative mutation is a CAG repeat expansion in exon 1 of the *HD* gene which translates into a polyglutamine tract in the huntingtin (Htt) protein (Huntington's Disease Collaborative Research Group, 1993). Pathologically, HD is

* Corresponding author: Jang-Ho J. Cha, MassGeneral Institute for Neurodegenerative Disease, Massachusetts General Hospital, 114 16th Street, Charlestown, MA 02129. Telephone: 001-617-724-1481, Fax: 001-617-724-1480, Email: cha@helix.mgh.harvard.edu.
Section Editor: Dr. Constantino Sotelo, CNRS UMR 7102, Universite Pierre et Marie Curie, 6eme etage, Bat B, Case 12, 9 Quai St Bernard, 75005 Paris, France

Conflict of interest statement: The authors declare that they have no competing interests.

characterized by generalized brain atrophy, and selective neuronal cell death predominantly in the striatum. Decreases in neurotransmitter receptors have been identified in HD striatum including glutamate, dopamine, γ-aminobutyric acid (GABA), and muscarinic cholinergic receptors. Presymptomatic HD patients have decreases in dopamine receptor levels as well as decreases in mRNA levels for dopamine D1 and dopamine D2 receptors and striatal neuropeptides such as preproenkephalin (PPE) (reviewed in Yohrling and Cha, 2002).

The R6/2 mouse model expresses only exon 1 of the human *HD* gene and displays selective decreases in dopamine D1, group I metabotropic glutamate receptors and PPE mRNA well before the onset of clinical symptoms, possibly contributing to their neurological decline (Mangiarini et al., 1996,Cha et al., 1998,Cha et al., 1999,Luthi-Carter et al., 2000). Furthermore, in other HD mouse models, there is down-regulation of neurotransmitter receptors and neuropeptides, particularly in those mice displaying an overt neurological phenotype (Menalled et al., 2000,Chan et al., 2002,Luthi-Carter et al., 2002,Kennedy et al., 2005).

The YAC128 transgenic mouse model was created with a yeast artificial chromosome (YAC) containing the entire human *HD* gene with 128 CAG repeats, including promoter regions (Slow et al., 2003). YAC128 mice display a progressive neurological phenotype, presenting with an initial hyperactivity and progressing to cognitive deficits and motor dysfunction (Van Raamsdonk et al., 2005). The motor deficit in the YAC128 mice is highly correlated with striatal neuronal loss, providing a structural correlate for the behavioral changes (Slow et al., 2003). To explore the role of glutamate in the development of symptoms, we examined glutamate receptors (GluRs) in brains taken from symptomatic 12 month old YAC128 transgenic mice and age-matched littermate controls using receptor binding autoradiography, mRNA *in situ* hybridization and immunoblotting for receptor proteins. We also analyzed GABA, adenosine and dopamine receptors, known to be affected in HD. We found increases in binding to NMDA, AMPA and group I and group II metabotropic glutamate receptors (mGluR) that were not wholly accounted for by increases in mRNA expression levels of receptor subunits. Subcellular fractionation revealed increased GluR localization in the synaptic fraction, which could suggest a receptor trafficking deficit in YAC128 mouse brains. The abnormal receptor binding appears specific for glutamate receptors as there were no changes in binding of GABA-A or GABA-B receptors, dopamine D1 or dopamine D2 receptors or adenosine A2a receptors. In contrast to the lack of changes in neurotransmitter receptor mRNA levels, there was a significant decrease in PPE mRNA.

MATERIALS AND METHODS

YAC72 and YAC128 mouse models

We have generated transgenic mouse lines using yeast artificial chromosomes (YACs) containing human genomic DNA spanning the full-length gene, including all regulatory elements. Transgenic mice express mutant huntingtin (Htt) containing 72 (YAC72) or 128 (YAC128) CAG repeats in a developmental and tissue-specific manner identical to that observed in Huntington's disease (HD) (Hodgson et al., 1999,Slow et al., 2003,Graham et al., 2006). YAC128 transgenic mice exhibit initial hyperactivity at 3 months of age, followed by hypokinesis at 12 months of age. The onset of a motor deficit on the rotarod is measurable at 6 months on age prior to the onset of neuronal loss at 9 months of age. YAC72 transgenic mice exhibit hyperactivity at 7 months of age and striatal medium spiny neuron degeneration is evident at 12 months of age. Thus, at 12 months of age, YAC72 mice are at an earlier symptomatic phase than 12 month YAC128 mice.

Tissue preparation

For YAC128 mice, six heterozygote symptomatic transgenic and six age-matched non-transgenic control mice were studied at 12 months of age for receptor analysis and mRNA *in situ* hybridization, and at 15 months of age for subcellular fractionation. Eight heterozygote transgenic and five age-matched non-transgenic control mice from the YAC72 line were studied at 12 months of age. All studies were conducted on coded samples by investigators blinded to genotype. Mice were sacrificed and brains were removed, snap-frozen in chilled isopentane and stored at −80°C. Sagittal cryostat sections (12 μm) were thaw-mounted onto glass slides and stored at −80°C and the same cohort of sections was suitable for receptor binding analysis and mRNA *in situ* hybridization. Frozen, dissected brain regions were used for subcellular fractionation and immunoblotting.

Receptor autoradiography

Autoradiographic studies were performed as described in (Benn et al., 2004). Briefly, for glutamate and GABA receptor studies, slides underwent a prewash in assay buffer for 30 min at 4°C and dried under a stream of cool air. Slides were then incubated for 45 min in [^{3}H]ligand in the presence or absence of displacers. Conditions were as follows: *Receptor assay*: concentration of [^{3}H]ligand; assay buffer, displacers present in the incubation assay, nonspecific "blank" condition. *α-Amino-3-hydroxy-5-methyl-4-isoxazolepropionic acid (AMPA):* 10 n*M* [^{3}H]AMPA; 50 m*M* Tris-HCl + 2.5 m*M* $CaCl_2$ + 30 m*M* potassium thiocyanate, pH 7.2 (Tris-HCl/$CaCl_2$/KSCN); displacers, none; blank, 1 m*M* glutamate. *N-methyl-D-aspartate* (*NMDA)*: 100 n*M* [^{3}H]glutamate; 50 m*M* Tris-acetate, pH 7.4; displacers, none; blank, 1 m*M* NMDA. *Group I metabotropic glutamate*: 100 n*M* [^{3}H]glutamate; Tris-HCl/$CaCl_2$/KSCN; displacers,100 μ*M* NMDA and 10 μ*M* AMPA; blank, 2.5 μ*M* quisqualate. *Group II metabotropic glutamate*: 100 n*M* [^{3}H]glutamate; Tris-HCl/$CaCl_2$/KSCN; displacers, 100 μ*M* NMDA, 10 μ*M* AMPA, and 2.5 μ*M* quisqualate; blank, 1 m*M* glutamate. The [3H] glutamate binding assays for metabotropic glutamate receptors can distinguish between group I and group II mGluR (Catania et al., 1994). *$GABA_A$*: 40 n*M* [^{3}H]GABA; 50 m*M* Tris-HCl + 2.5 m*M* $CaCl_2$, pH 7.4; displacers, 100 μ*M* baclofen; blank, 100 μ*M* isoguvacine. *$GABA_B$*: 40 n*M* [^{3}H]GABA; 50 m*M* Tris-HCl + 2.5 m*M* $CaCl_2$ pH 7.4; displacers, 100 μ*M* isoguvacine; blank, 100 μ*M* baclofen. All [^{3}H]ligands were obtained from Perkin Elmer (Wellesley, MA). After incubation in [^{3}H]ligand, slides were subjected to three rapid washes in cold buffer, one rapid wash in glutaraldehyde/acetone (2.5% vol/vol), and quickly dried under a stream of warm air.

Assays for D1-like and D2-like DA receptors used a buffer containing 25 m*M*Tris-HCl (pH 7.5), 100 m*M* NaCl, 1 m*M* $MgCl_2$, 1 μ*M* pargyline, and 10 mg/L ascorbate. For D1-like receptors, slides were incubated with 1.65 n*M* [^{3}H]SCH-23390 for 2.5 h. Nonspecific binding was defined in the presence 1 μ*M cis*-flupentixol). For D2-like receptors, slides were incubated with 180 p*M* [^{3}H]YM-09151–2 for 3 h. Nonspecific binding was defined in the presence 50 μ*M* DA. Adenosine A2a receptor binding was performed in 50 m*M* Tris-HCl, 10 m*M* $MgCl_2$, pH 7.4 and 2 U/mL adenosine deaminase. Slides were incubated with 50 n*M* [^{3}H] CGS21680 for 90 minutes. Non-specific binding was defined in the presence of 20 μ*M* chloroadenosine. For dopamine and adenosine receptor binding, following incubation in [^{3}H] ligand, slides were rinsed in cold buffer for 10 min, rinsed quickly in distilled water and dried under a stream of cool air.

For all receptor binding assays, slides and calibrated radioactive standards were apposed to Hyperfilm ^{3}H (Amersham, United Kingdom) for 1–3 months at 4°C. Films were developed and analyzed using a computer-based image analysis system (M1 Imaging Research, St Catharine's, Ontario, Canada). Image density corresponding to binding of [^{3}H]ligand was

converted to pmol/mg protein by using calibrated radioactive standards, and nonspecific binding was subtracted.

mRNA in situ hybridization

In situ hybridization was performed as described in (Benn et al., 2004). Briefly, frozen sections were thawed to room temperature then fixed for 10 min in 4% paraformaldehyde, washed twice in DEPC-PBS (0.1 *M* phosphate-buffered saline in DEPC-treated water) for 5 min each and dehydrated in graded ethanols from 70 – 100%. Sections were hybridized overnight with [^{35}S] end-labeled 45-mer oligonucleotide probes (800,000 dpm/μL) in sealed chambers humidified with 50% formamide/4X standard sodium citrate (SSC) water and washed three times in 1X SSC at 55°C. Slides were dehydrated with ethanol and exposed to Amersham β-max autoradiography film for one week. *In situ* hybridization signal was analyzed by measuring film densities using the M1 computer-based image analysis system. Probes used were antisense to ζ1, ε1 or ε2 NMDA receptor subunits (mouse orthologs of the NR1, NR2a and NR2b subunits) (15), GluR1, GluR2, GluR3, GluR4 subunits of the AMPA receptor (16), dopamine D1 and D2 receptors, adenosine A2a receptor and preproenkephalin (Benn et al., 2004). Controls were sections incubated with an excess (100 μ*M*) of unlabeled oligonucleotide.

Statistical analysis

A comparison of different groups (between genotypes and for each brain region) was performed on receptor binding and *in situ* data. We compared t-tests (one-way ANOVA) between genotypes in each region and compensated for multiple comparisons with Bonferroni-Dunn posthoc test. We additionally performed two-way ANOVA with Beonferroni-Dunn posthoc test. Significance level was $P<0.05$.

Real-time RT-PCR

Total RNA was extracted from mouse striatum with RNeasy Protect Mini Kit (Qiagen, Valencia, CA), and treated with Amplification Grade DNaseI (Invitrogen, Carlsbad, CA). First-strand cDNA was prepared from 1 μg of total RNA using SuperScript First-Strand Synthesis System for RT-PCR (Invitrogen). Approximately 700 pg of first-strand cDNA was used as template in real-time PCR reaction in a final volume of 25 μL. Mouse specific PPE primers and β-actin primers were designed to meet specific criteria by using Primer Express software (Perkin Elmer). The sequences for the PPE primers were 5′ TGC AGC TAC CGC CTG GTT 3′ and 5′ AGC TGT CCT TCA CAT TCC AGT GT 3′; and β-actin primers were 5′ ACGGCCAGGTCATCACTATTG 3′ and 5′ CAAGAAGGAAGGCTGGAAAAGA 3′. Real-time PCR was performed using the ABI PRISM 7000 Sequence Detection System and SYBR Green PCR Master Mix (Applied Biosystems, Foster City, CA). All samples were run in triplicate. Primary data analysis was performed using system software from Applied Biosystems. For each experimental sample, the amount of PPE mRNA and endogenous reference (β-actin) was determined from a standard curve. The standard curve was constructed with threefold serial dilutions of pooled cDNA samples (4500 pg to 170 pg) and was run in triplicate during every experiment. β-actin mRNA levels were used to control for template loading. The amount of PPE mRNA level was divided by the amount of β-actin mRNA level to obtain a relative PPE expression level. Statistical analysis of densitometry results were performed using a Students t-test and statistical significance was achieved at $P<0.05$.

Subcellular fractionation and immunoblotting

Subcellular fractionation was performed as described in (Dunah and Standaert, 2003). Briefly, striatum, frontal cortex, hippocampus and cerebellum were dissected from matched 15 month old YAC128 transgenic and wild-type control mouse brains. Dissections from 6 brains of each genotype were pooled, homogenized and subjected to sequential centrifuge steps at varying

g in sucrose buffers to obtain a range of fractions: H (total homogenate), P1 (nuclear debris), S2, P2 (crude synaptosomal membrane), S3, P3 (light membrane), LS1, LP1 (synaptosomal membrane), LS2, LP2 (synaptic vesicle enriched fraction). Pellet fractions are membrane-associated, soluble fractions are cytosolic. Fractions were quantified with the Bradford protein assay kit and stored as 20 μg aliquots at −80°C. Freshly thawed aliquots were loaded onto 10% SDS-PAGE gels, blotted on to PVDF membranes, immunoprobed and detected as described (Dunah et al., 1996). Manufacturer's guidelines for primary antibody concentration for immunoblotting were used. Antibodies to GluR1, GluR2/3, GluR4, NR1, NR2a, NR2b, α1 subunit of the GABA-A receptor, and MAb2166 (Htt) were all obtained from Chemicon (Temecula, CA). Antibodies to HIP1 and NR1 were from BD Biosciences Pharmingen (San Diego, CA). HRP conjugated secondary antibody dilutions were 1:10,000 (BioRad, Hercules, CA). Imaging and densitometry were performed on the Alpha Innotech FluorChem HD imaging platform (Alpha Innotech, San Leandro, CA). Statistical analysis of densitometry results were performed, comparing the two genotypes for each receptor protein within a particular region with one-way ANOVA (t-test) with Bonferroni-Dunn posthoc correction for multiple comparisons. Statistical significance was achieved at $P<0.05$.

RESULTS

Selective changes in glutamate receptor binding

We analyzed receptor binding autoradiography in the granule cell layer and molecular layer of the cerebellum, entorhinal cortex, CA1, CA3 and dentate gyrus of the hippocampus, inner cortex, outer cortex, striatum and thalamus in symptomatic 12 month old YAC128 mice and age-matched littermate controls. All studies were conducted on coded samples such that investigators were blinded to the genotype of the sample tissues. Receptor binding results are summarized in Table 1.

The anatomical pattern of NMDA receptor binding for both control and transgenic mice was similar to published autoradiographic studies (Cha et al., 1999), with the highest levels of binding in CA1, followed by other hippocampal regions, cortex and subcortical regions. Densitometric analysis of individual brain regions revealed a significant increase in NMDA receptor binding in the dentate gyrus of the hippocampus ($F(1,10)=5.26$; $P=0.045$) and the inner cortical layers ($F(1,11)=6.63$; $P=0.026$) in YAC128 transgenic mice (Figure 1, Table 1). Further statistical analysis of all the data to consider genotype effects by two-way ANOVA revealed a significant increase in NMDA binding in YAC128 mice compared to wild-type ($F(1,100)=17.9$, $P<0.001$) (whole brain, WB; Figure 1, Table 1). Interestingly, NMDA receptor binding shows a trend toward being increased in 12 month YAC72 transgenic mice compared to wild-type littermates ($F(1, 110)=3.107$, $P=0.081$) (whole brain, WB; Figure 2, Table 3), suggesting there may be a polyQ length dependent potentiation of NMDA receptor binding.

The anatomical pattern of AMPA binding in both control and transgenic mouse brain was also similar to published autoradiographic studies in mouse, with highest binding in hippocampal regions (Cha et al., 1999). There was a significant increase in AMPA binding in the transgenic when compared to the wild-type mice that was limited to the molecular cell layer of the cerebellum ($F(1,10)=12.35$; $P=0.006$) (Figure 1, Table 1). Furthermore, statistical analyses employing two-way ANOVA revealed an increase of AMPA receptor binding across all brain regions in YAC128 transgenic mice ($F(1,100)=11.06$; $P=0.001$). AMPA receptor binding was also significantly increased in YAC72 transgenic mice compared to wild-type mice by two-way ANOVA ($F(1,110)=9.093$, $P=0.003$), suggesting that AMPA receptor binding may be more sensitive to the gain-of-function conferred by an expanded polyQ tract than NMDA receptors (whole brain, WB; Figure 1, Table 3).

We observed no difference in binding to group I mGluR within any brain region analyzed in the YAC128 mouse brain (Figure 1, Table 1). However, there was a significant effect of genotype on binding of the ligand, which was increased overall in YAC128 transgenic mouse brains as compared to wild-type ($F(1,100)=6.14$; $P=0.015$). We observed a significant increase in binding of the ligand to group II mGluR in the dentate gyrus of the hippocampus ($F(1,10)=14.02$; $P=0.004$) in the YAC128 mouse brains, but two-way ANOVA revealed no difference in group II mGluR binding in transgenic YAC128 mouse brains when data from all brain regions are considered (Figure 1, Table 1).

No changes in non-glutamatergic receptor binding in YAC128 mice

Given the increases in glutamate receptor binding, we investigated other neurotransmitter receptors. Decreases in GABA receptor binding have been reported in human HD patient brains (Penney and Young, 1982). We therefore assessed GABA-A and GABA-B receptor binding profiles in the YAC128 transgenic mouse line. However, we found no changes in binding of ligand to GABA-A or GABA-B receptors in YAC128 transgenic mice compared to wild-type littermate control mice (Figure 3 and Table 1).

We also investigated the binding of striatal-enriched neurotransmitter receptors implicated in HD pathogenesis. Assessment of the dopaminergic receptors revealed no changes in dopamine D1- or D2-like receptor binding in the YAC128 transgenic mice compared to wild-type littermate controls (Figure 3, Table 1). Similarly, there were no changes in dopamine D1- or D2-like receptor binding in YAC72 mice (data not shown). As expected, the binding pattern of these receptors showed a striatal-enriched distribution for both wild-type and transgenic YAC128 mouse brains. We investigated the binding properties of another striatally enriched neurotransmitter receptor, the adenosine A2a receptor, which has been reported to be down-regulated in the R6/2 mouse model of HD (Cha et al., 1998,Cha et al., 1999). We observed no change in adenosine A2a receptor binding in transgenic mice compared to their control counterparts for either the YAC128 mouse line (Figure 3, Table 1) or in YAC72 line (data not shown). Together, these observations argue that neuronal degeneration in the striatum does not simply cause a corresponding decrease in neurotransmitter receptor density. Furthermore, the lack of change in non-glutamergic receptor binding highlights the specificity of the increases in binding to glutamate receptors in YAC128 transgenic mouse brains.

Increases in glutamate receptor binding are not explained by increases in glutamate receptor subunit mRNA expression

We have observed selective increases in glutamate receptor binding in the brains of YAC128 transgenic mice. Increases in receptor protein could result from increased mRNA levels. To investigate this possibility, we performed *in situ* hybridization for mRNA expression levels of the NMDA and AMPA receptor protein subunits (Figure 4 and Table 2).

We used probes specific for the ζ1, ε1 or ε2 NMDA receptor subunits (the mouse orthologs of rat NR1, NR2a and NR2b subunits) of the NMDA receptor. The anatomical pattern of mRNA expression of each subunit in both control and transgenic mouse brain was similar to published studies (Cha et al., 1998,Cha et al., 1999). We found no differences between transgenic and wild-type mice in mRNA expression levels in any brain region for the NR1, NR2a or NR2b subunits of the NMDA receptor (Figure 4, Table 2). Similarly, 2-way ANOVA revealed no effect of genotype on the mRNA expression level of any of the NR1, NR2a or NR2b subunit mRNA expression levels in YAC128 mice. Analysis of YAC72 mice also revealed no changes in any of the NR1, NR2a or NR2b subunit mRNA expression levels (data not shown). Therefore, increased transcription of NMDA receptor subunit mRNA is not responsible for the increase in NMDA-R binding.

We further probed the mRNA expression levels of the GluR1, GluR2, GluR3 and GluR4 subunits of the AMPA receptor (Figure 4, Table 2). The anatomical pattern of AMPA mRNA expression for all four subunits in both control and transgenic mouse brains was similar to published studies in rat (Keinanen et al., 1990). We found no differences in GluR1 mRNA expression in any of the brain regions, nor was it increased overall in transgenic mouse brains. We observed a significant increase in GluR2 limited to inner cortex ($F(1,11)=5.36$; $P=0.041$), striatum ($F(1,11)=12.72$; $P=0.004$) and thalamus ($F(1,11)=6.48$; $P=0.027$) in transgenic mice, but 2-way ANOVA revealed no effect of genotype on overall GluR2 expression. In contrast, 2-way ANOVA revealed a significant effect of genotype on overall GluR3 expression in YAC128 mice ($F(1,110)=6.172$; $P=0.015$), despite a lack of regional differences within the brain. We observed a significant effect of genotype on GluR4 mRNA expression, with expression being significantly increased in transgenic mice ($F(1,100)=11.06$; $P=0.001$). However, there was no increase in GluR4 mRNA levels in the molecular cell layer of the cerebellum, where this subtype is predominantly expressed. While there were increases in GluR2 mRNA in discrete brain regions, and overall increases in GluR3 and GluR4 mRNA levels, it appears unlikely that these could contribute to an increase in AMPA-R protein levels. GluR3 and GluR4 are expressed at very low levels in the brain and furthermore, the GluR2 subunit was increased only in 3 specific brain regions. Therefore, it appears unlikely that increases in mRNA levels of the AMPA receptor subunits alone are sufficient to cause the increases in AMPA receptor binding.

No changes in non-glutamergic receptor mRNA expression levels

The dopamine D1- and D2-like and adenosine A2a neurotransmitter receptors predominantly expressed in the striatum do not have altered binding in YAC128 transgenic mice. We sought to confirm whether the mRNA levels of these neurotransmitter receptors were also unchanged as they have previously been demonstrated to be altered in HD patient brains and other transgenic mouse models (reviewed in Yohrling and Cha, 2002). We found the mRNA expression of dopamine D1 and D2 receptors was predominant in the striatum in both YAC128 and control mice, as expected. We did not observe any differences in the mRNA levels of the D1 or D2 dopamine receptors in the striatum (Figure 5, Table 2). Similarly, the pattern of adenosine A2a mRNA expression appeared typical in both control and transgenic mice. Again, we observed no differences in mRNA expression levels of the A2a receptor in the striatum of YAC128 transgenic mice compared to control mice (Figure 5, Table 2), nor in the striatum of YAC72 mice compared to their wild-type littermate controls (data not shown).

Increased synaptic localization of glutamate receptors

A number of possible molecular mechanisms could underlie our observation of specific increases in glutamate receptor binding. Alterations of mRNA expression levels are insufficient to cause these increases in receptor binding, thus ruling out increased transcription as an underlying molecular mechanism. It is unclear if receptor binding measures only surface receptors; theoretically, receptor binding assays on tissue sections might also be labeling intracellular receptors. We therefore performed biochemical fractionation to determine the abundance and subcellular localization of glutamate receptor subunits in control and transgenic YAC128 mouse brains. These experiments were performed on homogenates prepared from pooled dissections of the striatum, hippocampus, cortex and cerebellum from wild-type and transgenic YAC128 mice. Fractions of particular interest were these from whole homogenates (H) (which indicate the total amount of the neurotransmitter receptor protein), the light membrane fraction (P3) (intracellular stores) and the synaptosomal fraction (LP1) (containing synaptic membranes and intracellular synaptic vesicles). There was insufficient tissue from the dissected brain regions to prepare a synaptic vesicle fraction (LP2). LP1 and P3 fractions were run in triplicate for densitometry analyses, and all fractions are shown for purposes of comparison (Figures 6 and 7).

There was more NMDA NR1 subunit protein in the LP1 fraction in fractions from striatum (P=0.002) and cortex (P=0.015) of transgenic mice, but no difference in the hippocampus or the cerebellum. NR2a protein levels were increased in the LP1 fraction of YAC128 mice compared to wild-type mice in cortex (P=0.006) and hippocampus (P=0.014) despite no difference in protein levels in the P3 fractions. In contrast, NR2a levels were actually decreased in the cerebellum (P=0.033). Similarly, NR2b protein levels were increased in LP1 fractions prepared from the cortex (P=0.002) and hippocampus (P=0.008) of YAC128 transgenic mice, but was unchanged in the striatum and cerebellum. Therefore, there were increases in NMDA receptor protein in the LP1 synaptic membrane fraction predominantly in the cortex and hippocampus, to a lesser extent in the striatum and no changes at all in the cerebellum (Figure 7). Thus, there were marked differences in the pattern of NMDA receptor subunit expression in the different brain regions.

As for NMDA receptor subunits, we found increases in AMPA receptor subunits protein in LP1 fractions from YAC128 transgenic mice (Figure 7). Overall, we observed significantly increased GluR1 receptor subunit protein in the hippocampus only (P=0.002). There was significantly increased GluR2/3 and GluR4 protein in the cortex (P<0.001 for GluR2/3 and P=0.001 for GluR4), in the hippocampus (GluR2/3, P=0.027) and in the cerebellum (GluR4, P=0.007). As for NMDA receptor subunit proteins, each brain region had a distinct pattern of increased/unchanged levels of AMPA receptor subunit proteins, which argues against generalized abnormalities in receptor protein control in YAC128 transgenic mouse brain. In contrast to the increases in glutamate receptor subunit proteins, we observed no significant differences in GABA-A receptor localization in LP1 fractions from YAC128 transgenic mice (Figures 6 and 7).

Blots were re-probed for the Htt protein. As expected, we saw a band corresponding to full-length endogenous murine Htt in both wild-type and transgenic YAC128 mice (Figure 7). We also saw a band corresponding to full-length mutant Htt in YAC128 mice in all fractions, resulting in an overload of Htt protein in subcellular fractions within YAC128 transgenic mouse brains. Blots were additionally re-probed using antibodies to huntingtin-interacting protein 1 (HIP1). We observed increases in HIP1 protein levels in the P3 fraction that were significant in the cortex (P=0.001) and striatum (P=0.032). Finally, we confirmed that equivalent amounts of protein were loaded in each fraction by re-probing blots with antibodies to beta-actin (Figures 6 and 7) and by staining protein gels with Coomassie Blue (data not shown).

Preproenkephalin is down-regulated in the YAC128 transgenic mice

The neuropeptide preproenkephalin (PPE) mRNA is decreased in striata of symptomatic and presymptomatic human HD patients (Augood et al., 1996). In addition, numerous mouse models of HD have decreases in PPE mRNA at presymptomatic time points, before the onset of a transgenic phenotype (Luthi-Carter et al., 2000,Menalled et al., 2000,Ariano et al., 2002,Luthi-Carter et al., 2002). Decreased expression of PPE mRNA may thus be an early sign of neuronal dysfunction due to the Huntington's disease mutation. We analyzed PPE mRNA levels in 12 month old YAC128 mice by mRNA *in situ* hybridization. PPE mRNA expression was predominantly in the striatum in both control and transgenic mice. We observed a significant decrease in PPE mRNA levels in the striata of 12 month old transgenic mice compared to wild-type littermate controls (Figure 8, Table 2). This decrease was confirmed by real-time RT-PCR (Figure 8).

DISCUSSION

Specific increases in NMDA and AMPA glutamate receptor binding in defined regions of YAC128 mouse brains occurred in the absence of corresponding mRNA changes, suggesting that increased transcription was not responsible for the receptor binding increases. Subcellular

fractionation revealed complex alterations of glutamate receptor subunit protein localization in synaptic membrane fractions limited to discrete brain regions in YAC128 transgenic mice. The abnormal increases in receptor binding and synaptic membrane localization were specific to glutamate receptors, as we found no changes in binding, mRNA expression or subcellular protein localization for GABA, dopamine or adenosine receptors. Finally, we found preproenkephalin mRNA was specifically down-regulated in YAC128 mice.

Glutamate receptors in HD

Intrastriatal administration of exogenous glutamate receptor agonists, particularly NMDA agonists, reproduces neuropathological features of HD (Beal et al., 1986,DiFiglia, 1990,Albin and Greenamyre, 1992). Enhancement of NMDA receptor-mediated synaptic currents and comprised calcium homeostasis has been reported in multiple cell and mouse models of HD in addition to the YAC128 mouse model (Cepeda et al., 2001,Laforet et al., 2001,Zeron et al., 2002,Gines et al., 2003,Li et al., 2003,Li et al., 2004,Zeron et al., 2004,Tang et al., 2005,Fan and Raymond, 2006,Shehadeh et al., 2006). Mutant Htt-potentiated NMDA receptor currents at the synapse in YAC72 striatal cell cultures are postulated to be due to an increase in NMDA receptors at the synaptic surface and a concomitant increase in receptor activity as mRNA expression levels were unchanged (Li et al., 2003), which correlates well with our findings. Interestingly, unpublished data (reported in (Fan and Raymond, 2006)) shows increased NMDA receptor subunit expression at the synaptic membrane of cultured medium striatal neurons from YAC72 mice, which could explain the enhanced current and toxicity. Furthermore, polyQ length dependent Htt-mediated potentiation of NMDA receptors in YAC128 striatal cell cultures has been reported to result in abnormal Ca^{2+} homeostasis and neuronal apoptosis (Tang et al., 2005,Graham et al., 2006,Shehadeh et al., 2006).

Enhanced NMDA receptor current does not correlate with the extent of sensitivity to excitotoxic insult. The R6/2 transgenic mouse model of HD exhibits an increased NMDA receptor mediated current and a decreased sensitivity to quinolinic acid excitotoxic insults (reviewed in Fan and Raymond, 2006). In contrast, sensitivity to glutamergic administration is increased in the YAC72 mouse model, which has enhanced striatal neuronal vulnerability to NMDA administration through increased Ca^{2+} influx (Zeron et al., 2002,Zeron et al., 2004). Interestingly, NMDA receptor binding is maintained or decreased in the R6/2 mouse model but is increased the YAC128 model, thus suggesting a molecular correlate for the difference in response to excitotoxic glutamergic insults.

NMDA receptor binding and synaptic localization abnormalities were most prominent in the hippocampus and the cortex. Aberrant NMDA receptor function in the context of long-term potentiation in the hippocampus and corticostriatal synapses have been reported in multiple models of HD (reviewed in Fan and Raymond, 2006). An elegant study examined the role of synaptic circuitry in BAC transgenic mice expressing a truncated mutant Htt fragment either in all forebrain neurons or only within the cortex (Gu et al., 2005). Progressive motor deficits and cortical neuropathology only occurred when mutant transgene expression is in multiple neuronal types, suggesting that cell-cell interactions between cortical and striatal neurons are critical for HD pathogenesis.

There were increases in binding to both groups I and II mGluRs in YAC128 transgenic mice. Metabotropic glutamate receptors are functionally neuromodulatory and are implicated in synaptic plasticity and cell death, particularly through NMDA receptor potentiation (Orlando et al., 2001, reviewed in Jayakar and Dikshit, 2004). Additionally, mGluRs have been proposed to modulate ionotropic glutamatergic synaptic transmission by regulating glutamate release. Interestingly, Taylor-Robinson and co-workers report increased glutamate levels in the striata of HD patients (Taylor-Robinson et al., 1996). Furthermore, HD patients have been reported to have dysmorphic dendritic arbors and spines in spiny striatal neurons, potentially increasing

the number of functional connections, thus facilitating neuronal excitability and excitotoxic cell death (Ferrante et al., 1991).

Disrupted post-translational control of glutamate receptors

A number of possible molecular mechanisms could underlie our observation of specific increases in glutamate receptor binding. Alterations of mRNA expression levels are insufficient to cause these increases in receptor binding, thus ruling out increased transcription as an underlying molecular mechanism. We found complex alterations in NMDA and AMPA receptor subunit protein levels in the synaptic membrane fraction that were unique to each brain region analyzed, predicting a complex alteration of glutamatergic neurotransmission in different regions of the YAC128 mouse brain. While there are some apparent discrepancies between the receptor binding data and the subcellular fractionation data, it is important to note that the receptor binding levels reflects the total number of receptors that can be bound, including intracellular receptors, and thus does not necessarily correlate with the protein levels at the synapse.

The abnormal glutamate receptor binding and presence in the synaptic fraction could be due to alterations in receptor trafficking or to disrupted control of post-translational modification of receptor subunits, such as phosphorylation. Further equally valid possibilities are that receptor mRNA and/or protein stability is altered or that the glutamate receptors are modulated post-translationally. Indeed, in R6/2 mice and a cell model, there are regionally specific alterations of NMDA receptors at multiple levels, including subunit mRNA levels, subunit phosphorylation and levels of anchoring proteins (Luthi-Carter et al., 2003,Song et al., 2003). Therefore, the molecular mechanism underlying glutamate receptor binding and synaptic localization abnormalities needs clarifying.

Striatal cell loss does not automatically alter neurotransmitter receptor levels

GABAergic striatal projection neurons degenerate in human HD patient brains and decreases in D1 and D2 dopaminergic receptors have been documented in human HD patient brains and transgenic mouse models (Penney and Young, 1982,Cha et al., 1998,Cha et al., 1999). In contrast to findings in the R6/2 model, we found no difference in GABA-A, GABA-B, D1-like dopamine, D2-like dopamine or A2a adenosine receptor binding in 12 month-old YAC128 transgenic mice. Similarly, we found no changes in mRNA expression levels for D1 dopamine, D2 dopamine or A2a adenosine receptors, nor in GABA-A protein levels in the LP1 fraction. Therefore, the lack of change in non-glutamate neurotransmitter receptors together with specific glutamate receptor increases suggests a selective molecular mechanism.

YAC128 mice exhibit a 15% reduction in striatal neuron number at 12 months of age (Slow et al., 2003). However, it is important to note that receptor binding assays measure receptor density and consequently is not a reliable determinant of the numbers of surviving cells. Thus, decreased numbers of striatal neurons would not necessarily produce decreased levels of receptor binding density. Hence, the observation that levels of binding to GABA-A, dopamine D1 and D2 receptors is unchanged in transgenic mice is not inconsistent with decreased numbers of striatal neurons, and could in fact represent a compensatory mechanism. Indeed, immunoblotting data suggest unchanged levels of receptor protein in the total homogenate fraction, although this has not been confirmed by densitometry analyses. While receptor binding levels appear unchanged at 12 months in YAC128 mice, it does not negate the possibility of altered receptor binding levels at other time points.

Transcriptional dysregulation of preproenkephalin mRNA levels

Previous work has revealed mRNA alterations, both in human patient brains and HD models (Augood et al., 1996,Cha et al., 1998,Cha et al., 1999,Luthi-Carter et al., 2000,Chan et al.,

2002,Luthi-Carter et al., 2002,Zucker et al., 2005). We found no differences in NR1, NR2a or NR2b, D1, D2 or A2a mRNA expression levels in YAC128 transgenic mice, arguing against a global transcriptional deficit. However, we observed a decrease in the preproenkephalin (PPE) mRNA levels, which agrees with well-documented decreases in other mouse models of HD and human HD patients (Augood et al., 1996,Luthi-Carter et al., 2000,Menalled et al., 2000,Ariano et al., 2002,Luthi-Carter et al., 2002). The decrease in PPE mRNA cannot be a simple consequence of neuronal loss, as the levels of other mRNA species have been maintained, or even increased in the striatum. This suggests the decrease in PPE mRNA could be due to a selective transcriptional deficit. YAC128 mice thus share with other mouse models the finding that preproenkephalin mRNA levels are decreased, supporting transcriptional dysregulation as a common pathogenic mechanism in HD.

Acknowledgements

We wish to thank Ghazaleh Sadri-Vakili, Anthone W. Dunah and Penny J. Hallett for helpful discussions and critical reading of the manuscript. This work was supported by grants from the Huntington's Disease Society of America Coalition for the Cure Program, Glendorn Foundation, Canadian Institutes of Health Research, the Michael Smith Foundation for Health Research and the National Institutes of Health (NIH NS38106, NS45242, AG13617).

References

Albin RL, Greenamyre JT. Alternative excitotoxic hypotheses. Neurology 1992;42:733–738. [PubMed: 1314341]

Ariano MA, Aronin N, Difiglia M, Tagle DA, Sibley DR, Leavitt BR, Hayden MR, Levine MS. Striatal neurochemical changes in transgenic models of Huntington's disease. J Neurosci Res 2002;68:716–729. [PubMed: 12111832]

Augood SJ, Faull RL, Love DR, Emson PC. Reduction in enkephalin and substance P messenger RNA in the striatum of early grade Huntington's disease: a detailed cellular in situ hybridization study. Neuroscience 1996;72:1023–1036. [PubMed: 8735227]

Beal MF, Kowall NW, Ellison DW, Mazurek MF, Swartz KJ, Martin JB. Replication of the neurochemical characteristics of Huntington's disease by quinolinic acid. Nature 1986;321:168–171. [PubMed: 2422561]

Benn CL, Farrell LA, Cha JH. Neurotransmitter receptor analysis in transgenic mouse models. Methods Mol Biol 2004;277:231–260. [PubMed: 15201460]

Cepeda C, Ariano MA, Calvert CR, Flores-Hernandez J, Chandler SH, Leavitt BR, Hayden MR, Levine MS. NMDA receptor function in mouse models of Huntington disease. J Neurosci Res 2001;66:525–539. [PubMed: 11746372]

Cha JH, Frey AS, Alsdorf SA, Kerner JA, Kosinski CM, Mangiarini L, Penney JB Jr, Davies SW, Bates GP, Young AB. Altered neurotransmitter receptor expression in transgenic mouse models of Huntington's disease. Philos Trans R Soc Lond B Biol Sci 1999;354:981–989. [PubMed: 10434296]

Cha JH, Kosinski CM, Kerner JA, Alsdorf SA, Mangiarini L, Davies SW, Penney JB, Bates GP, Young AB. Altered brain neurotransmitter receptors in transgenic mice expressing a portion of an abnormal human huntington disease gene. Proc Natl Acad Sci U S A 1998;95:6480–6485. [PubMed: 9600992]

Chan EY, Luthi-Carter R, Strand A, Solano SM, Hanson SA, DeJohn MM, Kooperberg C, Chase KO, DiFiglia M, Young AB, Leavitt BR, Cha JH, Aronin N, Hayden MR, Olson JM. Increased huntingtin protein length reduces the number of polyglutamine-induced gene expression changes in mouse models of Huntington's disease. Hum Mol Genet 2002;11:1939–1951. [PubMed: 12165556]

DiFiglia M. Excitotoxic injury of the neostriatum: a model for Huntington's disease. Trends in Neurosciences 1990;13:286–289. [PubMed: 1695405]

Dunah AW, Standaert DG. Subcellular segregation of distinct heteromeric NMDA glutamate receptors in the striatum. J Neurochem 2003;85:935–943. [PubMed: 12716425]

Dunah AW, Yasuda RP, Wang YH, Luo J, Davila-Garcia M, Gbadegesin M, Vicini S, Wolfe BB. Regional and ontogenic expression of the NMDA receptor subunit NR2D protein in rat brain using a subunit-specific antibody. J Neurochem 1996;67:2335–2345. [PubMed: 8931465]

Fan MM, Raymond LA. N-Methyl-d-aspartate (NMDA) receptor function and excitotoxicity in Huntington's disease. Prog Neurobiol. 2006

Ferrante RJ, Kowall NW, Richardson EP Jr. Proliferative and degenerative changes in striatal spiny neurons in Huntington's disease: a combined study using the section-Golgi method and calbindin D28k immunocytochemistry. J Neurosci 1991;11:3877–3887. [PubMed: 1836019]

Gines S, Ivanova E, Seong IS, Saura CA, MacDonald ME. Enhanced Akt signaling is an early pro-survival response that reflects N-methyl-D-aspartate receptor activation in Huntington's disease knock-in striatal cells. J Biol Chem 2003;278:50514–50522. [PubMed: 14522959]

Graham RK, Slow EJ, Deng Y, Bissada N, Lu G, Pearson J, Shehadeh J, Leavitt BR, Raymond LA, Hayden MR. Levels of mutant huntingtin influence the phenotypic severity of Huntington disease in YAC128 mouse models. Neurobiol Dis 2006;21:444–455. [PubMed: 16230019]

Gu X, Li C, Wei W, Lo V, Gong S, Li SH, Iwasato T, Itohara S, Li XJ, Mody I, Heintz N, Yang XW. Pathological cell-cell interactions elicited by a neuropathogenic form of mutant Huntingtin contribute to cortical pathogenesis in HD mice. Neuron 2005;46:433–444. [PubMed: 15882643]

Hodgson JG, Agopyan N, Gutekunst CA, Leavitt BR, LePiane F, Singaraja R, Smith DJ, Bissada N, McCutcheon K, Nasir J, Jamot L, Li XJ, Stevens ME, Rosemond E, Roder JC, Phillips AG, Rubin EM, Hersch SM, Hayden MR. A YAC mouse model for Huntington's disease with full-length mutant huntingtin, cytoplasmic toxicity, and selective striatal neurodegeneration. Neuron 1999;23:181–192. [PubMed: 10402204]

Huntington's Disease Collaborative Research Group. A novel gene containing a trinucleotide repeat that is expanded and unstable on Huntington's disease chromosomes. Cell 1993;72:971–983. [PubMed: 8458085]

Jayakar SS, Dikshit M. AMPA receptor regulation mechanisms: future target for safer neuroprotective drugs. Int J Neurosci 2004;114:695–734. [PubMed: 15204061]

Keinanen K, Wisden W, Sommer B, Werner P, Herb A, Verdoorn TA, Sakmann B, Seeburg PH. A family of AMPA-selective glutamate receptors. Science 1990;249:556–560. [PubMed: 2166337]

Kennedy L, Shelbourne PF, Dewar D. Alterations in dopamine and benzodiazepine receptor binding precede overt neuronal pathology in mice modelling early Huntington disease pathogenesis. Brain Res 2005;1039:14–21. [PubMed: 15781041]

Laforet GA, Sapp E, Chase K, McIntyre C, Boyce FM, Campbell M, Cadigan BA, Warzecki L, Tagle DA, Reddy PH, Cepeda C, Calvert CR, Jokel ES, Klapstein GJ, Ariano MA, Levine MS, DiFiglia M, Aronin N. Changes in cortical and striatal neurons predict behavioral and electrophysiological abnormalities in a transgenic murine model of Huntington's disease. J Neurosci 2001;21:9112–9123. [PubMed: 11717344]

Li L, Fan M, Icton CD, Chen N, Leavitt BR, Hayden MR, Murphy TH, Raymond LA. Role of NR2B-type NMDA receptors in selective neurodegeneration in Huntington disease. Neurobiol Aging 2003;24:1113–1121. [PubMed: 14643383]

Li L, Murphy TH, Hayden MR, Raymond LA. Enhanced striatal NR2B-containing N-methyl-D-aspartate receptor-mediated synaptic currents in a mouse model of Huntington disease. J Neurophysiol 2004;92:2738–2746. [PubMed: 15240759]

Luthi-Carter R, Apostol BL, Dunah AW, DeJohn MM, Farrell LA, Bates GP, Young AB, Standaert DG, Thompson LM, Cha JH. Complex alteration of NMDA receptors in transgenic Huntington's disease mouse brain: analysis of mRNA and protein expression, plasma membrane association, interacting proteins, and phosphorylation. Neurobiol Dis 2003;14:624–636. [PubMed: 14678777]

Luthi-Carter R, Strand A, Peters NL, Solano SM, Hollingsworth ZR, Menon AS, Frey AS, Spektor BS, Penney EB, Schilling G, Ross CA, Borchelt DR, Tapscott SJ, Young AB, Cha JH, Olson JM. Decreased expression of striatal signaling genes in a mouse model of Huntington's disease. Hum Mol Genet 2000;9:1259–1271. [PubMed: 10814708]

Luthi-Carter R, Strand AD, Hanson SA, Kooperberg C, Schilling G, La Spada AR, Merry DE, Young AB, Ross CA, Borchelt DR, Olson JM. Polyglutamine and transcription: gene expression changes shared by DRPLA and Huntington's disease mouse models reveal context-independent effects. Hum Mol Genet 2002;11:1927–1937. [PubMed: 12165555]

Mangiarini L, Sathasivam K, Seller M, Cozens B, Harper A, Hetherington C, Lawton M, Trottier Y, Lehrach H, Davies SW, Bates GP. Exon 1 of the HD gene with an expanded CAG repeat is sufficient

to cause a progressive neurological phenotype in transgenic mice. Cell 1996;87:493–506. [PubMed: 8898202]

Menalled L, Zanjani H, MacKenzie L, Koppel A, Carpenter E, Zeitlin S, Chesselet MF. Decrease in striatal enkephalin mRNA in mouse models of Huntington's disease. Exp Neurol 2000;162:328–342. [PubMed: 10739639]

Orlando LR, Alsdorf SA, Penney JB Jr, Young AB. The role of group I and group II metabotropic glutamate receptors in modulation of striatal NMDA and quinolinic acid toxicity. Exp Neurol 2001;167:196–204. [PubMed: 11161608]

Penney JB Jr, Young AB. Quantitative autoradiography of neurotransmitter receptors in Huntington disease. Neurology 1982;32:1391–1395. [PubMed: 6292789]

Shehadeh J, Fernandes HB, Zeron Mullins MM, Graham RK, Leavitt BR, Hayden MR, Raymond LA. Striatal neuronal apoptosis is preferentially enhanced by NMDA receptor activation in YAC transgenic mouse model of Huntington disease. Neurobiol Dis 2006;21:392–403. [PubMed: 16165367]

Slow EJ, van Raamsdonk J, Rogers D, Coleman SH, Graham RK, Deng Y, Oh R, Bissada N, Hossain SM, Yang YZ, Li XJ, Simpson EM, Gutekunst CA, Leavitt BR, Hayden MR. Selective striatal neuronal loss in a YAC128 mouse model of Huntington disease. Hum Mol Genet 2003;12:1555–1567. [PubMed: 12812983]

Song C, Zhang Y, Parsons CG, Liu YF. Expression of polyglutamine-expanded huntingtin induces tyrosine phosphorylation of N-methyl-D-aspartate receptors. J Biol Chem 2003;278:33364–33369. [PubMed: 12810713]

Tang TS, Slow E, Lupu V, Stavrovskaya IG, Sugimori M, Llinas R, Kristal BS, Hayden MR, Bezprozvanny I. Disturbed Ca2+ signaling and apoptosis of medium spiny neurons in Huntington's disease. Proc Natl Acad Sci U S A 2005;102:2602–2607. [PubMed: 15695335]

Taylor-Robinson SD, Weeks RA, Bryant DJ, Sargentoni J, Marcus CD, Harding AE, Brooks DJ. Proton magnetic resonance spectroscopy in Huntington's disease: evidence in favour of the glutamate excitotoxic theory. Mov Disord 1996;11:167–173. [PubMed: 8684387]

Van Raamsdonk JM, Pearson J, Slow EJ, Hossain SM, Leavitt BR, Hayden MR. Cognitive dysfunction precedes neuropathology and motor abnormalities in the YAC128 mouse model of Huntington's disease. J Neurosci 2005;25:4169–4180. [PubMed: 15843620]

Yohrling, GJ.; Cha, J-HJ. Striatal neurochemistry of Hungtington's disease. In: Bates, GP., et al., editors. Huntington's disease. Oxford University Press; Oxford: 2002. p. 276-308.

Zeron MM, Fernandes HB, Krebs C, Shehadeh J, Wellington CL, Leavitt BR, Baimbridge KG, Hayden MR, Raymond LA. Potentiation of NMDA receptor-mediated excitotoxicity linked with intrinsic apoptotic pathway in YAC transgenic mouse model of Huntington's disease. Mol Cell Neurosci 2004;25:469–479. [PubMed: 15033175]

Zeron MM, Hansson O, Chen N, Wellington CL, Leavitt BR, Brundin P, Hayden MR, Raymond LA. Increased sensitivity to N-methyl-D-aspartate receptor-mediated excitotoxicity in a mouse model of Huntington's disease. Neuron 2002;33:849–860. [PubMed: 11906693]

Zucker B, Luthi-Carter R, Kama JA, Dunah AW, Stern EA, Fox JH, Standaert DG, Young AB, Augood SJ. Transcriptional dysregulation in striatal projection- and interneurons in a mouse model of Huntington's disease: neuronal selectivity and potential neuroprotective role of HAP1. Hum Mol Genet 2005;14:179–189. [PubMed: 15548548]

Abbreviations

AMPA

Alpha-amino-3-hydroxy-5-methyl-4-isoxazolepropionic acid

GABA

γ-aminobutyric acid

GluR

Glutamate receptor

GluR1–4
: Subunits of the AMPA glutamate receptor

HD
: Huntington's disease

HIP1
: Huntingtin-interacting protein 1

Htt
: Huntingtin

mGluR
: Metabotropic glutamate receptor

NMDA
: N-methyl-D-aspartate

NR1
: NR2a, NR2b, Subunits of the NMDA glutamate receptor

PPE
: Preproenkephalin

YAC
: Yeast artificial chromosome

YAC72/YAC128
: Transgenic mouse model of Huntington's disease made using a YAC containing the full length human gene and 72/128 CAG repeats respectively

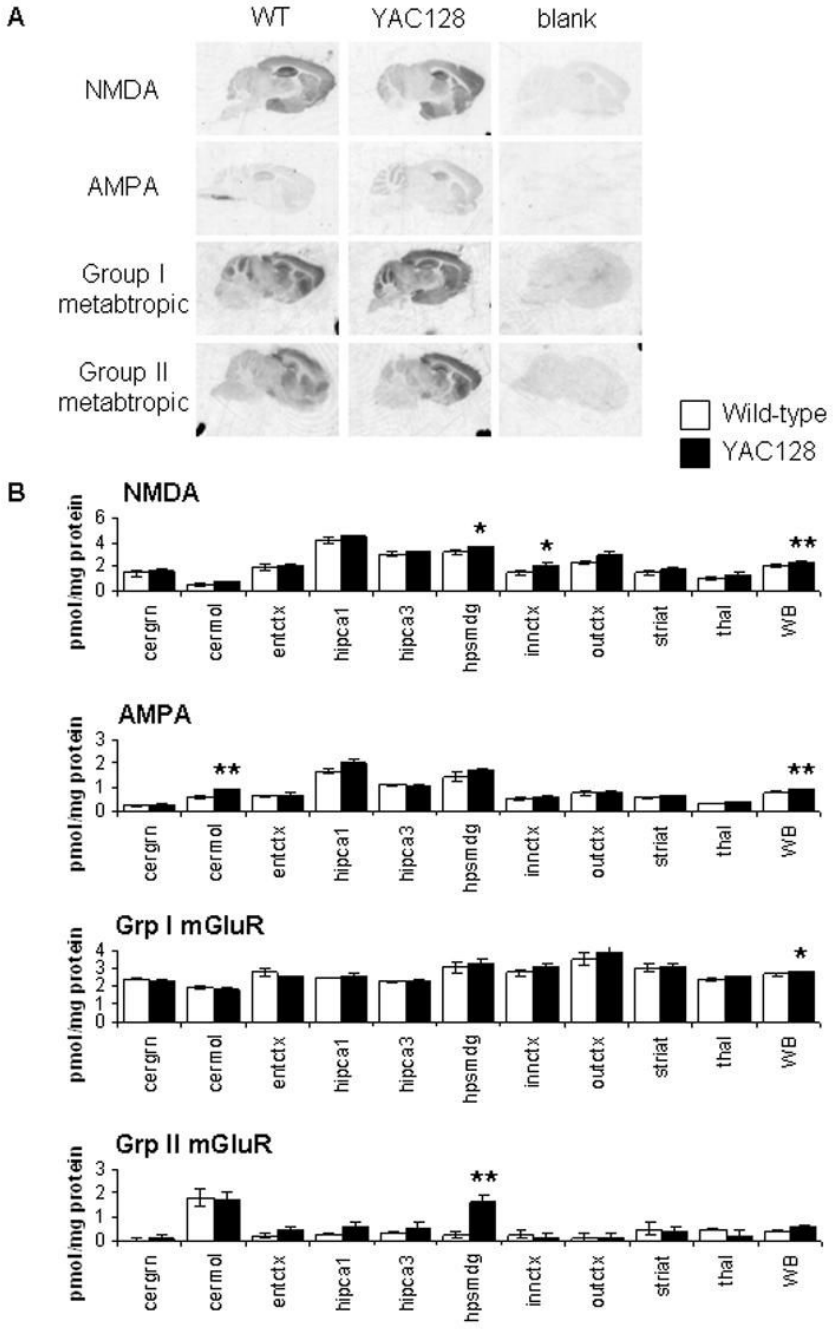

Figure 1. Increased glutamate receptor binding in YAC128 mice

(a) Glutamate receptor binding appears dark in representative images of control (WT) and transgenic (YAC128) mice for NMDA, AMPA, group I and group II metabotropic glutamate receptors and blank sections demonstrate the specificity of the binding. **(b)** Graphs show the densitometric analysis of film images converted into to picomoles of [^{3}H]ligand bound per milligram protein (pmol/mg protein). Regions analyzed were the granule cell layer of the cerebellum (cergrn), molecular layer of the cerebellum (cermol), entorhinal cortex (entctx), hippocampal CA1 (hipca1), CA3 (hipca3) and dentate gyrus (hpsmdg), deep layers of the frontal cortex (innctx), superficial layers of the frontal cortex (outctx), striatum (striat), thalamus (thal) and whole brain (WB). * $p<0.05$, ** $p<0.01$.

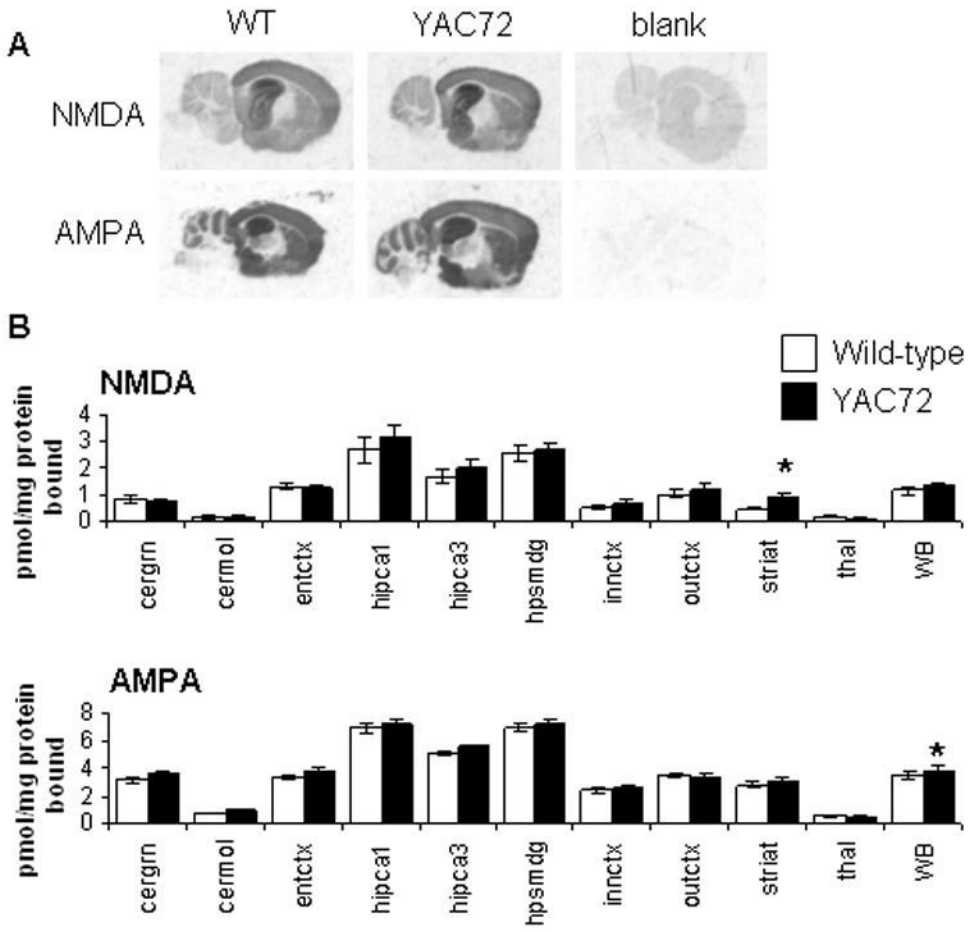

Figure 2. Increased glutamate receptor binding in YAC72 mice

(a) Representative images of glutamate receptor are shown for control (WT) and transgenic (YAC72) mice for NMDA and AMPA receptors. **(b)** Graphs show the densitometric analysis of film images converted into to picomoles of [^{3}H]ligand bound per milligram protein (pmol/mg protein). The same regions are analyzed as for the YAC128 mice (Figure 1b). Open bars represent control mice, filled bars represent transgenic mice. * $p<0.05$, ** $p<0.01$.

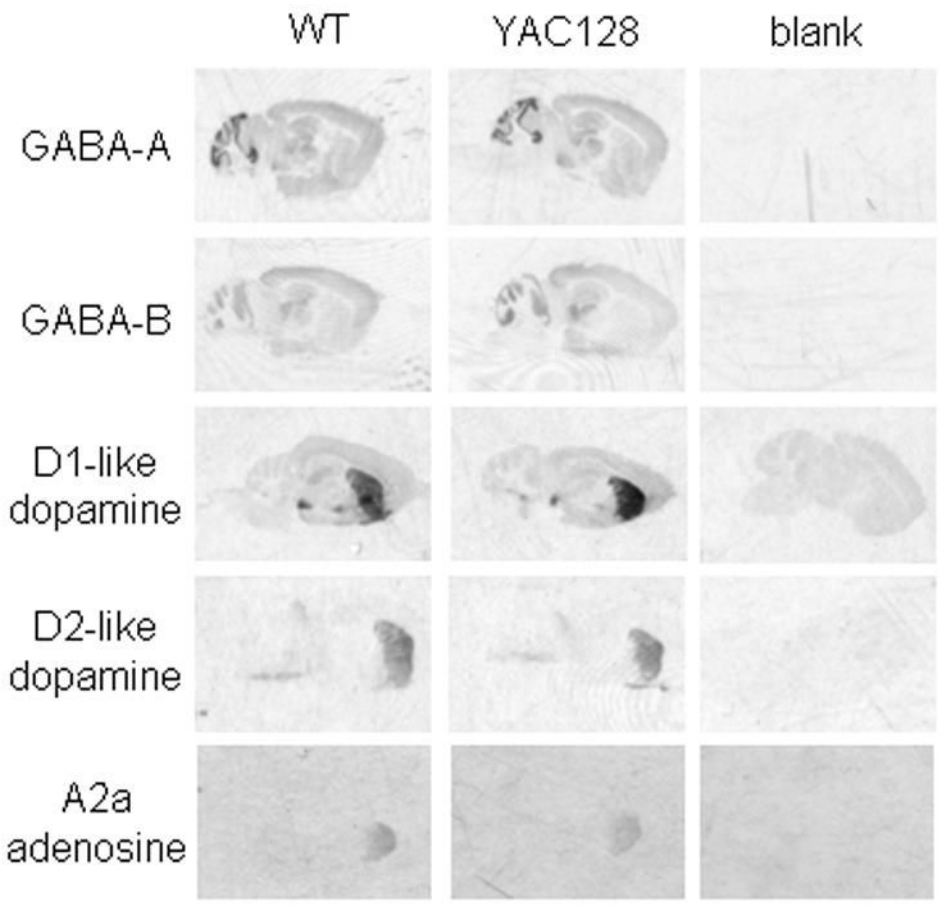

Figure 3. Non-glutamate receptor binding is unchanged in YAC128 mice

(a) Receptor binding appears dark in representative images of control (WT) and transgenic (YAC128) mice for GABA-A, GABA-B, D1-like dopamine, D2-like dopamine, and A2a adenosine receptors and blank sections demonstrate the specificity of the binding.

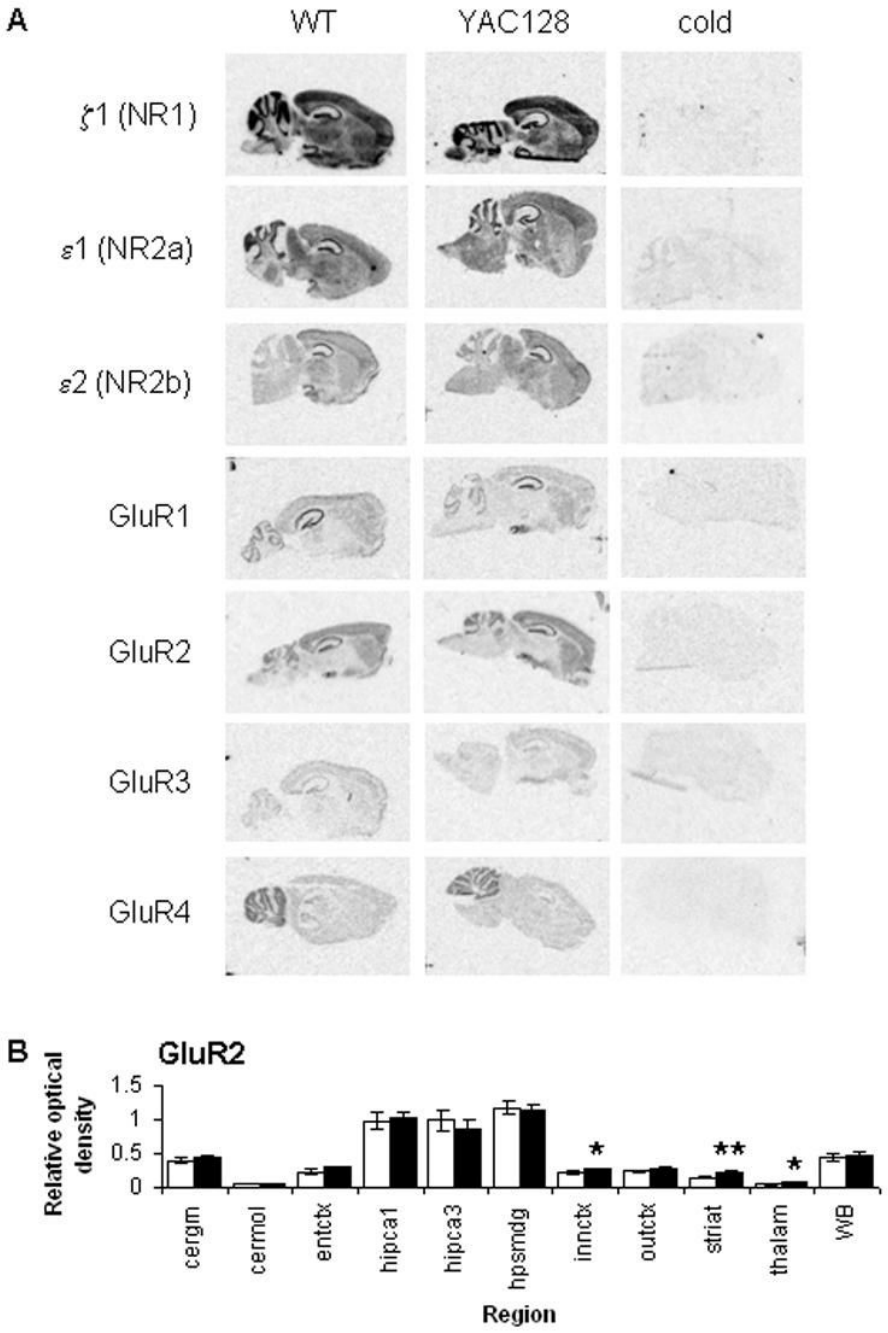

Figure 4. Glutamate receptor subunit mRNA expression levels do not explain the increase in glutamate receptor binding in YAC128 mice

(a) Receptor subunit mRNA expression appears dark in representative images of control (WT) and transgenic (YAC128) mice for the NR1, NR2a, NR2b subunits of the NMDA receptor and the GluR1, GluR2, GluR3 and GluR4 subunits of the AMPA receptor, with "cold" sections showing the specificity of the labeling. **(b)** Densitometric quantitation of the GluR2 subunit mRNA levels is shown. Regions analyzed were the granule cell layer of the cerebellum (cergrn), molecular layer of the cerebellum (cermol), entorhinal cortex (entctx), hippocampal CA1 (hipca1), CA3 (hipca3) and dentate gyrus (hpsmdg), deep layers of the frontal cortex (innctx), superficial layers of the frontal cortex (outctx), striatum (striat), thalamus (thal) and

whole brain (WB). Open bars represent control mice, filled bars represent transgenic mice. * $p<0.05$, ** $p<0.01$.

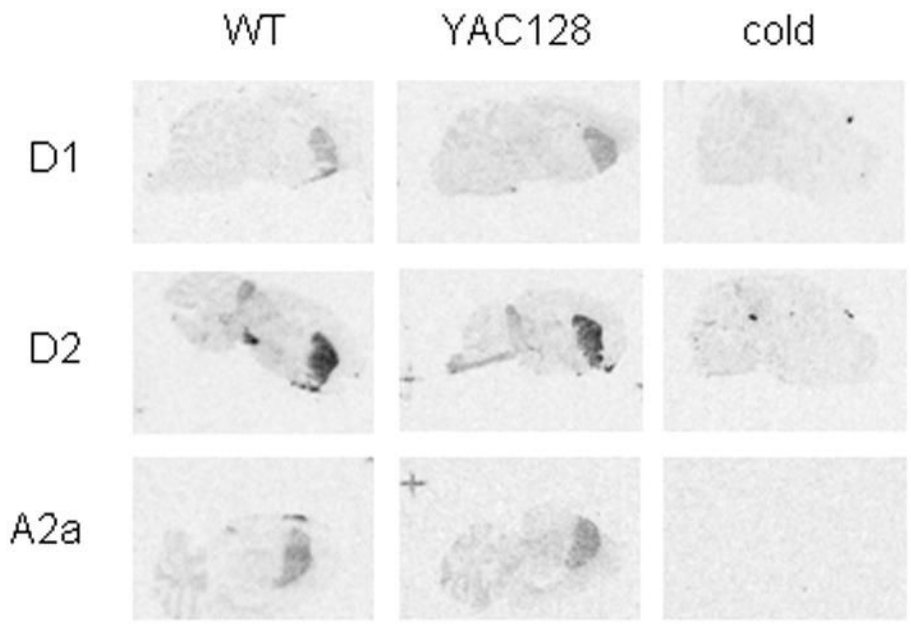

Figure 5. No change in non-glutamatergic receptor subunit mRNA expression levels in YAC128 mice

(a) Representative images of control (WT) and transgenic (YAC128) mice, with "cold" sections showing the specificity of the labeling are shown for D1 dopamine receptor, D2 dopamine receptor and A2a adenosine receptor mRNA species. Densitometric analysis revealed no differences in striatal mRNA levels for dopamine D1-or D2-like dopamine receptors, or A2a adenosine receptors (Table 2).

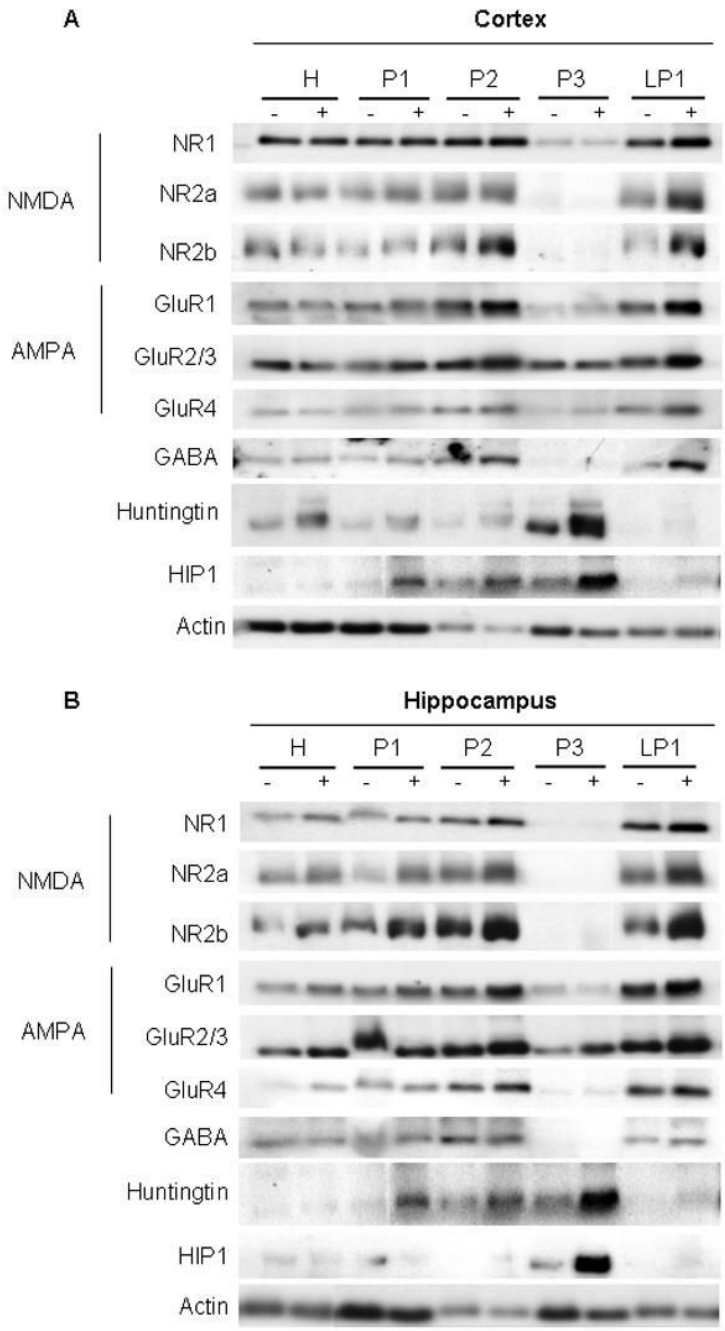

Figure 6. Subcellular fractionation analysis suggests an increase in glutamate receptor subunits in the synaptic membrane of YAC128 transgenic mice

Membrane bound subcellular fractions (20 μg) from WT (−) and YAC128 transgenic (+) dissected brain regions (striatum, cortex, hippocampus and cerebellum) were used for Western blotting. Shown are representative blots from **(a)** the cortex and **(b)** the hippocampus–regions which have the most alterations in glutamate receptor binding. Antibodies used recognize the NMDA receptor subunits NR1, NR2a, NR2b; the AMPA receptor subunits GluR1, GluR2/3, GluR4; GABA(A)a1 subunit of the GABA receptor, Htt Interacting Protein 1 (HIP1), Htt (MAb2166), with actin and Coomassie-blue stained gels (not shown) as loading controls. Key:

H (total homogenate), P1 (nucleus and debris), P2 (crude synaptosomal membrane), P3 (light membrane) and LP1 (synaptosomal membrane).

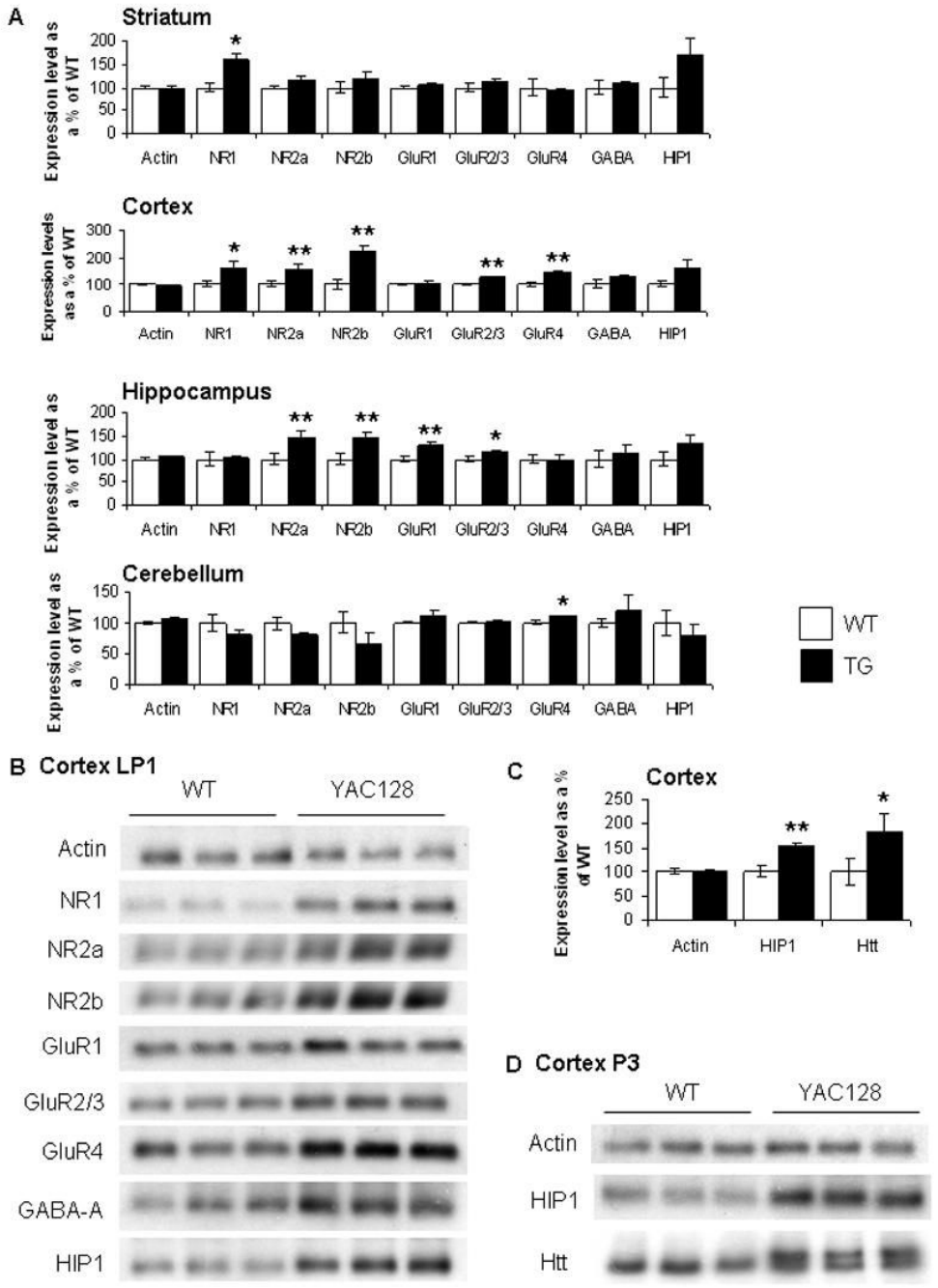

Figure 7. Quantitation of LP1 and P3 subcellular fractions shows an increase in glutamate receptor subunits in the synaptic membrane of YAC128 transgenic mice

Membrane bound subcellular fractions (20 μg) from WT (−) and YAC128 transgenic (+) dissected brain regions (striatum, cortex, hippocampus and cerebellum) were used for Western blotting. Antibodies used recognize the NMDA receptor subunits NR1, NR2a, NR2b; the AMPA receptor subunits GluR1, GluR2/3, GluR4; GABA(A)a1 subunit of the GABA receptor, Htt Interacting Protein 1 (HIP1), Htt (MAb2166), with actin and Coomassie-blue stained gels (not shown) as loading controls. **(a)** Densitometry was performed on LP1 samples loaded in triplicate for the striatum, cortex, hippocampus and the cerebellum. Graphs show the amounts of each protein from the fractions which are expressed as a percentage of wild-type

(WT) mice of the same brain region. Open bars represent control wild-type mice, filled bars represent transgenic YAC128 mice. * P<0.05, ** P<0.01, *** P<0.001. **(b)** Representative blots used for densitometry for the LP1 (synaptosomal membrane) fraction from cortex – the region which has the most alterations in glutamate receptor binding – are shown. Fractions were made from dissected regions from wild-type (WT) and transgenic (YAC128) brains. Samples are loaded in triplicate. **(c)** Densitometry was performed on P3 samples loaded in triplicate for the striatum, cortex, hippocampus and the cerebellum. Shown is the data from the cortex, a region which shows dramatic changes in the amounts of each protein from the transgenic fractions which are expressed as a percentage of wild-type (WT) mice of the same brain region. Open bars represent control mice, filled bars represent transgenic mice (YAC128). * P<0.05, ** P<0.01. **(d)** Representative blots used for densitometry of actin, HIP1 and Htt (MAb2166) in the P3 fraction from the cortex, the region which shows the most changes.

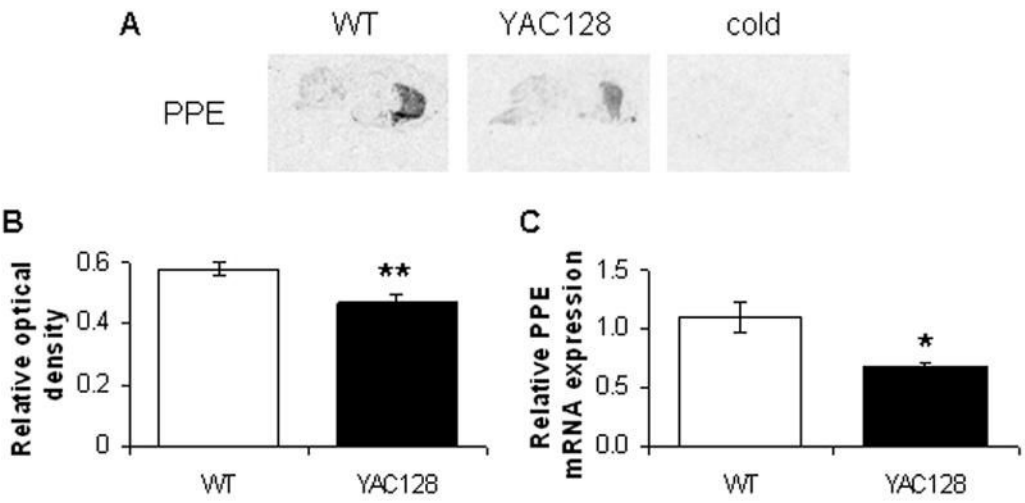

Figure 8. Preproenkephalin mRNA levels are decreased in YAC128 mice

(a) Preproenkephalin (PPE) mRNA levels appear dark in representative autoradiographs from control (WT) and transgenic (YAC128) mice. The decrease in intensity of signal is clearly visible in the YAC128 mouse brain section. **(b)** Densitometric analysis was performed on the striatum only as shown in the graph. **(c)** The graph shows relative PPE mRNA expression levels by real-time RT-PCR, using beta-actin mRNA levels to control for template loading. Open bars represent control mice, filled bars represent transgenic mice. * $p<0.05$, ** $p<0.01$.

Table 1

Receptor binding data in YAC128 mice

Receptor assay	Effect	Posthoc p value 2-way ANOVA	Region	Genotype	Binding ± SD pmol/mg protein	Posthoc p value 1-way ANOVA
NMDA	Genotype	**<0.0001**	cergm	control	14.28 ± 5.65	
			cergm	transgenic	15.98 ± 4.05	
	Genotype × Region	0.896	cermol	control	4.58 ± 4.26	
			cermol	transgenic	6.72 ± 2.81	
			entctx	control	18.76 ± 6.20	
			entctx	transgenic	19.89 ± 4.41	
			hipCA1	control	41.30 ± 5.56	
			hipCA1	transgenic	44.81 ± 2.93	
			hipCA3	control	29.89 ± 4.98	
			hipCA3	transgenic	31.48 ± 3.36	
			hspdg	control	31.89 ± 5.19	
			hspdg	transgenic	36.58 ± 1.73	**0.045**
			innctx	control	14.59 ± 3.70	
			innctx	transgenic	21.08 ± 6.11	**0.026**
			outctx	control	23.54 ± 3.87	
			outctx	transgenic	28.90 ± 6.48	
			striat	control	14.26 ± 3.08	
			striat	transgenic	17.71 ± 3.29	
			thal	control	9.82 ± 3.82	
			thal	transgenic	13.27 ± 2.23	
AMPA	Genotype	**0.001**	cergm	control	0.19 ± 0.04	
			cergm	transgenic	0.25 ± 0.06	
	Genotype × Region	0.143	cermol	control	0.62 ± 0.13	
			cermol	transgenic	0.87 ± 0.12	**0.006**
			entctx	control	0.65 ± 0.08	
			entctx	transgenic	0.69 ± 0.16	
			hipCA1	control	1.68 ± 0.34	
			hipCA1	transgenic	2.05 ± 0.37	
			hipCA3	control	1.1 ± 0.14	
			hipCA3	transgenic	1.02 ± 0.23	
			hspdg	control	1.43 ± 0.46	
			hspdg	transgenic	1.73 ± 0.12	
			innctx	control	0.53 ± 0.15	
			innctx	transgenic	0.62 ± 0.21	
			outctx	control	0.74 ± 0.18	
			outctx	transgenic	0.75 ± 0.20	
			striat	control	0.58 ± 0.13	
			striat	transgenic	0.67 ± 0.08	
			thal	control	0.31 ± 0.06	
			thal	transgenic	0.38 ± 0.04	
Group I mGluR	Genotype	**0.015**	cergm	control	2.42 ± 0.08	
			cergm	transgenic	2.33 ± 0.12	
	Genotype × Region	**0.024**	cermol	control	1.89 ± 0.22	
			cermol	transgenic	1.81 ± 0.15	
			entctx	control	2.81 ± 0.50	
			entctx	transgenic	2.58 ± 0.09	
			hipCA1	control	2.49 ± 0.10	
			hipCA1	transgenic	2.60 ± 0.19	
			hipCA3	control	2.28 ± 0.16	
			hipCA3	transgenic	2.35 ± 0.13	
			hspdg	control	3.06 ± 0.96	
			hspdg	transgenic	3.28 ± 0.57	

Receptor assay	Effect	Posthoc p value 2-way ANOVA	Region	Genotype	Binding ± SD pmol/mg protein	Posthoc p value 1-way ANOVA
			innctx	control	2.76 ± 0.29	
			innctx	transgenic	3.06 ± 0.53	
			outctx	control	3.55 ± 0.81	
			outctx	transgenic	3.86 ± 1.07	
			striat	control	3.03 ± 0.57	
			striat	transgenic	3.13 ± 0.53	
			thal	control	2.40 ± 0.20	
			thal	transgenic	2.56 ± 0.19	
Group II mGluR	Genotype	0.320	cergm	control	0.01 ± 0.13	
			cergm	transgenic	0.11 ± 0.22	
	Genotype × Region	0.928	cermol	control	1.78 ± 0.92	
			cermol	transgenic	1.76 ± 0.73	
			entctx	control	0.17 ± 0.30	
			entctx	transgenic	0.43 ± 0.43	
			hipCA1	control	0.26 ± 0.13	
			hipCA1	transgenic	0.61 ± 0.43	
			hipCA3	control	0.31 ± 0.11	
			hipCA3	transgenic	0.53 ± 0.49	
			hspdg	control	0.21 ± 0.41	
			hspdg	transgenic	1.63 ± 0.83	**0.004**
			innctx	control	0.26 ± 0.52	
			innctx	transgenic	0.09 ± 0.63	
			outctx	control	0.11 ± 0.47	
			outctx	transgenic	0.08 ± 0.63	
			striat	control	0.48 ± 0.60	
			striat	transgenic	0.39 ± 0.48	
			thal	control	0.47 ± 0.13	
			thal	transgenic	0.16 ± 0.69	
GABA-A	Genotype	0.275	cergm	control	76.28 ± 5.45	
			cergm	transgenic	77.08 ± 5.67	
	Genotype × Region	0.986	cermol	control	23.13 ± 2.78	
			cermol	transgenic	22.68 ± 1.04	
			entctx	control	19.49 ± 2.19	
			entctx	transgenic	20.70 ± 1.19	
			hipCA1	control	22.47 ± 2.75	
			hipCA1	transgenic	23.00 ± 2.28	
			hipCA3	control	15.53 ± 2.00	
			hipCA3	transgenic	14.93 ± 1.83	
			hspdg	control	23.39 ± 2.26	
			hspdg	transgenic	25.05 ± 2.30	
			innctx	control	12.89 ± 2.26	
			innctx	transgenic	17.20 ± 1.50	
			outctx	control	17.34 ± 3.15	
			outctx	transgenic	21.83 ± 2.56	
			striat	control	12.48 ± 1.14	
			striat	transgenic	11.71 ± 0.70	
			thal	control	10.81 ± 1.65	
			thal	transgenic	12.66 ± 2.38	
D1-like	Genotype	0.910	striat	control	5.38 ± 1.54	
			striat	transgenic	5.29 ± 0.98	
D2-like	Genotype	0.860	striat	control	2.54 ± 0.44	
			striat	transgenic	2.59 ± 0.55	

Receptor assay	Effect	Posthoc p value 2-way ANOVA	Region	Genotype	Binding ± SD pmol/mg protein	Posthoc p value 1-way ANOVA
A2a	Genotype	0.965	striat striat	control transgenic	0.19 ± 0.09 0.19 ± 0.04	

Table 2

Optical density data from mRNA *in situ* hybridization

Receptor assay	Effect	ANOVA p value	Region	Genotype	Relative Optical Density ± S.D.	Posthoc p value
NMDA NR1	Genotype	0.851	cergrn	Control	0.69 ± 0.13	
			cergrn	transgenic	0.69 ± 0.16	
	Genotype × Region	0.989	cermol	Control	0.11 ± 0.04	
			cermol	transgenic	0.11 ± 0.04	
			entctx	Control	0.27 ± 0.05	
			entctx	transgenic	0.30 ± 0.11	
			hipCA1	Control	0.48 ± 0.13	
			hipCA1	transgenic	0.47 ± 0.08	
			hipCA3	Control	0.58 ± 0.16	
			hipCA3	transgenic	0.53 ± 0.17	
			hspdg	Control	0.59 ± 0.17	
			hspdg	transgenic	0.51 ± 0.22	
			innctx	Control	0.30 ± 0.06	
			innctx	transgenic	0.27 ± 0.08	
			outctx	Control	0.27 ± 0.08	
			outctx	transgenic	0.22 ± 0.08	
			striat	Control	0.21 ± 0.05	
			striat	transgenic	0.17 ± 0.07	
			thal	Control	0.19 ± 0.07	
			thal	transgenic	0.22 ± 0.06	
NMDA NR2a	Genotype	0.395	cergrn	Control	0.45 ± 0.12	
			cergrn	transgenic	0.45 ± 0.09	
	Genotype × Region	0.997	cermol	Control	0.11 ± 0.03	
			cermol	transgenic	0.11 ± 0.01	
			entctx	control	0.17 ± 0.04	
			entctx	transgenic	0.20 ± 0.03	
			hipCA1	control	0.46 ± 0.11	
			hipCA1	transgenic	0.49 ± 0.12	
			hipCA3	control	0.41 ± 0.05	
			hipCA3	transgenic	0.39 ± 0.08	
			hspdg	control	0.52 ± 0.13	
			hspdg	transgenic	0.53 ± 0.14	
			innctx	control	0.24 ± 0.05	
			innctx	transgenic	0.23 ± 0.01	
			outctx	control	0.17 ± 0.02	
			outctx	transgenic	0.19 ± 0.03	
			striat	control	0.12 ± 0.02	
			striat	transgenic	0.13 ± 0.01	
			thal	control	0.18 ± 0.03	
			thal	transgenic	0.21 ± 0.04	
NMDA NR2b	Genotype	0.581	cergrn	control	0.11 ± 0.03	
			cergrn	transgenic	0.12 ± 0.04	
	Genotype × Region	0.904	cermol	control	0.04 ± 0.01	
			cermol	transgenic	0.04 ± 0.01	
			entctx	control	0.13 ± 0.02	
			entctx	transgenic	0.15 ± 0.04	
			hipCA1	control	0.44 ± 0.10	
			hipCA1	transgenic	0.50 ± 0.15	
			hipCA3	control	0.49 ± 0.12	
			hipCA3	transgenic	0.46 ± 0.18	
			hspdg	control	0.51 ± 0.12	
			hspdg	transgenic	0.48 ± 0.12	
			innctx	control	0.14 ± 0.03	
			innctx	transgenic	0.13 ± 0.03	

Receptor assay	Effect	ANOVA p value	Region	Genotype	Relative Optical Density ± S.D.	Posthoc p value
			outctx	control	0.12 ± 0.02	
			outctx	transgenic	0.11 ± 0.03	
			striat	control	0.08 ± 0.01	
			striat	transgenic	0.10 ± 0.02	
			thal	control	0.09 ± 0.02	
			thal	transgenic	0.12 ± 0.01	
AMPA GluR1	Genotype	0.537	cergrn	control	0.47 ± 0.07	
			cergrn	transgenic	0.40 ± 0.11	
	Genotype × Region	0.901	cermol	control	0.05 ± 0.03	
			cermol	transgenic	0.05 ± 0.02	
			entctx	control	0.10 ± 0.02	
			entctx	transgenic	0.10 ± 0.02	
			hipCA1	control	0.83 ± 0.21	
			hipCA1	transgenic	0.82 ± 0.23	
			hipCA3	control	0.67 ± 0.22	
			hipCA3	transgenic	0.58 ± 0.15	
			hspdg	control	0.98 ± 0.21	
			hspdg	transgenic	1.04 ± 0.09	
			innctx	control	0.10 ± 0.01	
			innctx	transgenic	0.09 ± 0.01	
			outctx	control	0.09 ± 0.01	
			outctx	transgenic	0.08 ± 0.02	
			striat	control	0.10 ± 0.01	
			striat	transgenic	0.12 ± 0.03	
			thal	control	0.03 ± 0.01	
			thal	transgenic	0.03 ± 0.01	
AMPA GluR2	Genotype	0.481	cergrn	control	0.40 ± 0.12	
			cergrn	transgenic	0.44 ± 0.05	
	Genotype × Region	0.882	cermol	control	0.06 ± 0.03	
			cermol	transgenic	0.04 ± 0.01	
			entctx	control	0.24 ± 0.07	
			entctx	transgenic	0.30 ± 0.03	
			hipCA1	control	0.98 ± 0.28	
			hipCA1	transgenic	1.04 ± 0.18	
			hipCA3	control	1.00 ± 0.37	
			hipCA3	transgenic	0.87 ± 0.30	
			hspdg	control	1.18 ± 0.25	
			hspdg	transgenic	1.14 ± 0.22	
			innctx	control	0.22 ± 0.05	
			innctx	transgenic	0.28 ± 0.03	**0.041**
			outctx	control	0.24 ± 0.05	
			outctx	transgenic	0.28 ± 0.02	
			striat	control	0.15 ± 0.05	
			striat	transgenic	0.23 ± 0.03	**0.004**
			thal	control	0.05 ± 0.02	
			thal	transgenic	0.07 ± 0.01	**0.027**
AMPA GluR3	Genotype	**0.015**	cergrn	control	0.23 ± 0.03	
			cergrn	transgenic	0.22 ± 0.02	
	Genotype × Region	0.965	cermol	control	0.02 ± 0.01	
			cermol	transgenic	0.03 ± 0.02	
			entctx	control	0.11 ± 0.03	
			entctx	transgenic	0.14 ± 0.03	
			hipCA1	control	0.28 ± 0.08	
			hipCA1	transgenic	0.33 ± 0.09	
			hipCA3	control	0.31 ± 0.11	

Receptor assay	Effect	ANOVA p value	Region	Genotype	Relative Optical Density ± S.D.	Posthoc p value
			hipCA3	transgenic	0.34 ± 0.13	
			hspdg	control	0.37 ± 0.10	
			hspdg	transgenic	0.41 ± 0.14	
			innctx	control	0.12 ± 0.03	
			innctx	transgenic	0.17 ± 0.02	
			outctx	control	0.07 ± 0.01	
			outctx	transgenic	0.09 ± 0.03	
			striat	control	0.07 ± 0.01	
			striat	transgenic	0.09 ± 0.03	
			thal	control	0.05 ± 0.02	
			thal	transgenic	0.06 ± 0.02	
AMPA GluR4	Genotype	**0.001**	cergrn	control	0.48 ± 0.07	
			cergrn	transgenic	0.50 ± 0.07	
	Genotype × Region	0.143	cermol	control	0.10 ± 0.02	
			cermol	transgenic	0.10 ± 0.02	
			entctx	control	0.10 ± 0.02	
			entctx	transgenic	0.11 ± 0.02	
			hipCA1	control	0.16 ± 0.05	
			hipCA1	transgenic	0.18 ± 0.05	
			hipCA3	control	0.19 ± 0.06	
			hipCA3	transgenic	0.17 ± 0.06	
			hspdg	control	0.28 ± 0.08	
			hspdg	transgenic	0.30 ± 0.08	
			innctx	control	0.10 ± 0.02	
			innctx	transgenic	0.12 ± 0.03	
			outctx	control	0.11 ± 0.01	
			outctx	transgenic	0.12 ± 0.03	
			striat	control	0.06 ± 0.02	
			striat	transgenic	0.08 ± 0.03	
			thal	control	0.05 ± 0.02	
			thal	transgenic	0.09 ± 0.02	
D1 dopamine	Genotype	0.528	striat	control	0.09 ± 0.02	
			striat	transgenic	0.08 ± 0.02	
D2 dopamine	Genotype	0.634	striat	control	0.24 ± 0.04	
			striat	transgenic	0.26 ± 0.07	
A2a adenosine	Genotype	0.099	striat	control	0.07 ± 0.02	
			striat	transgenic	0.10 ± 0.03	
Preproenkephalin	Genotype	**0.008**	striat	control	0.58 ± 0.05	
			striat	transgenic	0.47 ± 0.08	

Table 3

Receptor binding data in YAC72 mice

Receptor assay	Effect	Posthoc p value	Region	Genotype	Binding ± SD (pmol/mg protein bound)	Posthoc p value
NMDA	Genotype	0.081	cergrn	control	0.83 ± 0.33	
			cergrn	transgenic	0.78 ± 0.17	
			cermol	control	0.17 ± 0.11	
			cermol	transgenic	0.18 ± 0.13	
			entctx	control	1.28 ± 0.21	
			entctx	transgenic	1.20 ± 0.32	
			hipCA1	control	2.69 ± 1.11	
			hipCA1	transgenic	3.19 ± 1.11	
			hipCA3	control	1.67 ± 0.47	
			hipCA3	transgenic	2.02 ± 0.78	
			hpsmdg	control	2.55 ± 0.67	
			hpsmdg	transgenic	2.67 ± 0.67	
			innctx	control	0.48 ± 0.24	
			innctx	transgenic	0.70 ± 0.40	
			outctx	control	1.02 ± 0.25	
			outctx	transgenic	1.17 ± 0.68	
			striat	control	0.45 ± 0.10	
			striat	transgenic	0.92 ± 0.45	**0.021**
			thal	control	0.18 ± 0.10	
			thal	transgenic	0.11 ± 0.17	
AMPA	Genotype	**0.003**	cergrn	control	3.15 ± 0.50	
			cergrn	transgenic	3.64 ± 0.42	
			cermol	control	0.80 ± 0.17	
			cermol	transgenic	0.93 ± 0.13	
			entctx	control	3.35 ± 0.44	
			entctx	transgenic	3.88 ± 0.44	
			hipCA1	control	6.82 ± 0.71	
			hipCA1	transgenic	7.25 ± 0.71	
			hipCA3	control	5.10 ± 0.29	
			hipCA3	transgenic	5.52 ± 0.36	**0.042**
			hpsmdg	control	7.00 ± 0.65	
			hpsmdg	transgenic	7.27 ± 0.64	
			innctx	control	2.44 ± 0.29	
			innctx	transgenic	2.59 ± 0.41	
			outctx	control	3.51 ± 0.43	
			outctx	transgenic	3.38 ± 0.70	
			striat	control	2.78 ± 0.57	
			striat	transgenic	3.09 ± 0.58	
			thal	control	0.59 ± 0.19	
			thal	transgenic	0.52 ± 0.23	